Nonradiative Dielectric Waveguide for Millimeter-Wave Integrated Circuits

TSUKASA YONEYAMA, MEMBER, IEEE, AND SHIGEO NISHIDA, SENIOR MEMBER, IEEE

Abstract—**A nonradiative dielectric waveguide is proposed in which dielectric strips are sandwiched between two parallel metal plates separated by a distance smaller than half a wavelength. Though the structure is substantially the same as that of the H-guide, it is based on a quite different principle of operation. This dielectric guide is particularly applicable in millimeter-wave integrated circuits, since it is not only small in size, but also allows bends and junctions to be incorporated into the circuits with very little radiation and interference. A design diagram is given. Losses and coupling coefficients of the strips are calculated, as well. Some basic circuit components, such as 90° and 180° bends and T-junctions, made of polystyrene strips, are measured to confirm their usefulness in millimeter-wave integrated circuits.**

I. Introduction

IN THE millimeter-wave region of the spectrum, various dielectric waveguides [1] have been proposed as possible substitutes for rather lossy microstrips and striplines. Although inherent losses of dielectric waveguides such as image guides [2] and insular guides [3] are reasonably small, additional radiation losses at curved sections are often above tolerable levels. The trapped image guide [4] utilizes a metal trough to reflect back radiated waves and has succeeded in reducing losses at 90° bends. But, the bulky trough does not seem practical in integrated-circuit applications.

Having these factors in mind, we propose a nonradiative dielectric waveguide. The structure resembles Tischer's H-guide [5], but the principle of operation is quite different, as will be made clear in the next section. Since this guide can almost completely suppress radiation and interference, it can be used to great advantage in millimeter-wave integrated circuits. Preliminary measurements of some basic circuit components have also been made at 50 GHz.

II. Principle of Operation

As is well known, if two parallel metal plates are separated by a distance smaller than half a wavelength, electromagnetic waves with the electric field parallel to the plates cannot propagate between them because of their cutoff property. However, if dielectric strips of a proper dielectric constant are brought in, as shown in Fig. 1, the cutoff is eliminated and waves are able to propagate freely along the strips, whether they be straight or curved. Since radiated waves, if any, decay outside the strips, bends and junctions can easily be incorporated into complicated integrated circuits. This is the principle of operation of the nonradiative dielectric waveguide. In this connection, we should remember that as for the H-guide, the sidewall separation is made much larger than half a wavelength to realize low-loss propagation, rather than to suppress radiated waves.

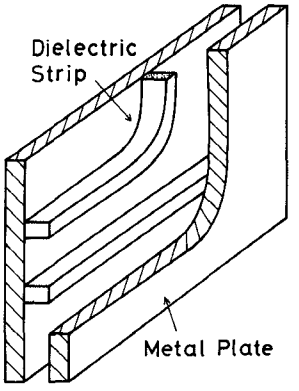

Fig. 1. Basic strip structure in nonradiative dielectric waveguide, held between two parallel metal plates separated by a distance smaller than half a wavelength.

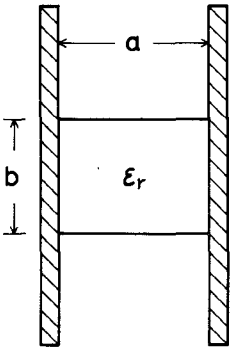

Fig. 2. Cross-sectional view of a straight dielectric strip in nonradiative dielectric waveguide.

To express the principle of operation mathematically, we will consider a straight strip as shown in Fig. 2. The width of the strip is a, the thickness is b, and the relative dielectric constant is ϵ_r. The analysis can be considerably facilitated, if we note that hybrid modes in the nonradiative guide can be viewed as resulting from TM surface waves propagating in the infinite slab of the same material and the same thickness as the strip and bouncing back and forth between the sidewalls. Specifically, the cutoff of the strip is given by

$$\lambda_{gn}=2a, \qquad n=0, 1,... \tag{1}$$

Manuscript received April 6, 1981; revised June 29, 1981.

The authors are with the Research Institute of Electrical Communication, Tohoku University, Katahira 2-chome, 1-1, Sendai, Japan 980.

0018-9480/81/1100-1188$00.75 ©1981 IEEE

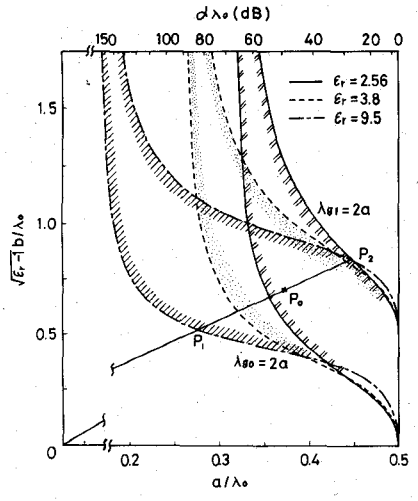

Fig. 3. Design diagram showing regions of the single-mode operation for strips of alumina ($\epsilon_r=9.5$), fused quartz ($\epsilon_r=3.8$), and polystyrene ($\epsilon_r=2.56$). Attenuation of radiated waves is marked on the upper abscissa. Points P_0, P_1, and P_2, and a straight line passing through them are for determining bandwidth in Section IV.

as implied previously [6], where λ_{gn} is the guide wavelength of the TM_n slab mode. The equation for λ_{gn} is

$$\lambda_{gn}=\frac{\lambda_0}{\sqrt{\epsilon_r-(\lambda_0 q_n/2\pi)^2}} \tag{2}$$

where λ_0 is the free-space wavelength and q_n is the nth solution of the characteristic equations [7]

$$\frac{q_n}{\epsilon_r}\tan\left(\frac{q_n b}{2}\right)-\sqrt{(\epsilon_r-1)\left(\frac{2\pi}{\lambda_0}\right)^2-q_n^2}=0, \qquad n \text{ even} \tag{3a}$$

$$\frac{q_n}{\epsilon_r}\cot\left(\frac{q_n b}{2}\right)+\sqrt{(\epsilon_r-1)\left(\frac{2\pi}{\lambda_0}\right)^2-q_n^2}=0, \qquad n \text{ odd}. \tag{3b}$$

Referring to (1), the condition for the single-mode operation is written as

$$\lambda_0,\lambda_{g1}>2a>\lambda_{g0} \tag{4}$$

where λ_{g0} and λ_{g1} are the guide wavelengths of the fundamental and second TM slab modes, respectively, and the free-space wavelength λ_0 is included to insure suppression of radiated waves. Calculation of (4) is made for alumina ($\epsilon_r=9.5$), fused quartz ($\epsilon_r=3.8$), and polystyrene ($\epsilon_r=2.56$), and plotted in Fig. 3. The single-mode operation is guaranteed in the region bounded by curves $\lambda_{g0}=2a$ and $\lambda_{g1}=2a$, and, in part, by a vertical line at $a/\lambda_0=0.5$. In the left of the region, no mode at all propagates, while in the right, multimode propagation may occur. The second mode in the widthwise direction has to be taken into account, when ϵ_r is larger than four, as is the case for alumina. But the second mode is not launched in the guide if the excitation is symmetrical.

Also marked on the upper abscissa is the attenuation of radiated waves in one free-space wavelength which is given

$$\alpha\lambda_0=54.6\sqrt{(\lambda_0/2a)^2-1}\ [\text{dB}]. \tag{5}$$

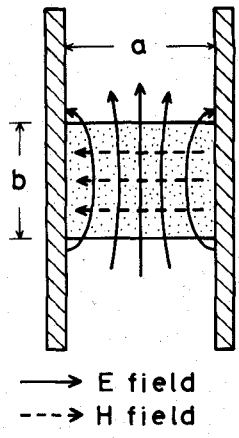

Fig. 4. Typical field lines in a cross-sectional plane of nonradiative dielectric waveguide.

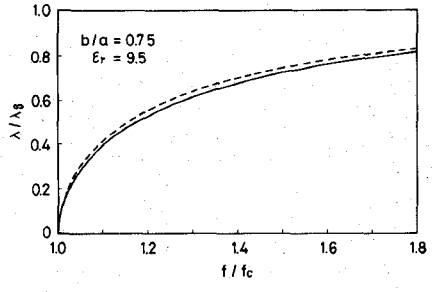

Fig. 5. Dispersion curves of nonradiative alumina waveguide (solid curve) and alumina-filled metal waveguide (dotted curve). Aspect ratio is $b/a=0.75$.

This is derived by considering that radiated waves in the nonradiative guide decay just as the TE_{10} mode does in a rectangular metal waveguide under cutoff. The above equation is helpful for estimating the magnitude of interference among circuit components by radiated waves. For instance, in the case of $a/\lambda_0=0.45$, we have $\alpha\lambda_0=26$ dB. This indicates that the strips can be arranged in a close spacing of one wavelength, if tolerance of 26 dB is permitted for interference.

For reference, field lines in a cross-sectional plane are depicted in Fig. 4. They are similar to those in a metal waveguide except for evanescent fringes near the surfaces of the strip.

III. Dispersion Characteristics

The dispersion curve of a nonradiative guide is very nearly identical to that of a metal waveguide filled with the dielectric material which is the same as that of the strip, as is seen in Fig. 5. The solid curve is calculated for alumina and the aspect ratio $b/a=0.75$. The ordinate is the ratio of the wavelength λ in the dielectric material to the guide wavelength λ_g and the abscissa is the ratio of frequency f to the cutoff frequency f_c.

Considering this, the nonradiative guide can be regarded as a dielectric-filled metal waveguide which does not need the top and bottom metal plates which are major sources of conduction loss. Although the dispersion characteristics are substantially similar, bandwidths of the single-mode opera-

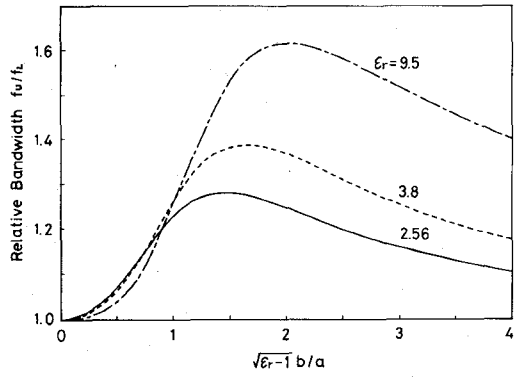

Fig. 6. Relative bandwidths of the single-mode operation for strips of alumina ($\epsilon_r=9.5$), fused quartz ($\epsilon_r=3.8$), and polystyrene ($\epsilon_r=2.56$).

tion are different for the two waveguides, as will be discussed in the next section.

IV. Bandwidth of Single-Mode Operation

Fig. 3 is also very convenient for schematically determining bandwidth of the single-mode operation. We will demonstrate this for an alumina strip. If values of a/λ_0 and $\sqrt{\epsilon_r-1}\,b/\lambda_0$ are specified for a strip, we can locate the corresponding point P_0 in Fig. 3. Then, if a line is drawn passing through P_0 and the origin O (notice that the abscissa is shortened in Fig. 3), we can find intersections P_1 and P_2 on the boundary curves. The relative bandwidth, which is defined by the ratio f_U/f_L of the upper and lower ends of the frequency region under consideration, is determined by the ratio between the lengths $\overline{OP_2}$ and $\overline{OP_1}$. The relative bandwidth takes a value of 1.6 for the case demonstrated. The value is large enough to cover U band from 40 to 60 GHz or V band from 50 to 75 GHz.

Fig. 6 shows the relative bandwidth as a function of the ratio $\sqrt{\epsilon_r-1}\,b/a$. The maximum values are 1.62, 1.39, and 1.28 for alumina, fused quartz, and polystyrene, respectively. The larger the dielectric constant, the wider the bandwidth achievable. Thus the alumina strips are particularly favorable for a wide bandwidth of operation.

V. Transmission Loss

Transmission loss α_t of a nonradiative guide consists of conduction loss α_c of the sidewalls and dielectric loss α_d of the strip. The constitutent losses can be obtained theoretically by the conventional techniques of approximation [8].

Fig. 7 shows the calculated losses of a specific alumina strip, 2 mm in width and 1.5 mm in thickness, designed for the U band. Material parameters are assumed to be $\tan\delta=10^{-4}$ for alumina and $\sigma=5.8\times10^7$ S/m for the copper plates. The transmission loss is almost constant over the U band except for very near the cutoff, where the losses show a sharp increase. The cutoffs of the fundamental and second modes are at 38.2 and 61.5 GHz, respectively.

Additional loss data are included in Table I for comparison purposes, along with those of insular guides [9]. Two cases ($a/\lambda_0=0.45$, $\sqrt{\epsilon_r-1}\,b/\lambda_0=0.45$ and $a/\lambda_0=0.45$, $\sqrt{\epsilon_r-1}\,b/\lambda_0=0.7$) are presented. The latter, though larger in size, is less lossy than the insular guides. This is due to the reduction of conduction loss peculiar to fields polarized

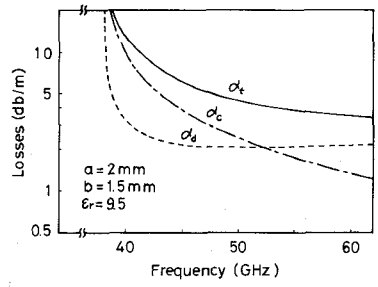

Fig. 7. Transmission loss α_t, conduction loss α_c, and dielectric loss α_d of nonradiative dielectric waveguide, designed for the U band.

TABLE I
Theoretical Characteristics of Nonradiative Guide and Insular Guide

Description		Freq. (GHz)	Width a(mm)	Thickness b(mm)	λ_g (mm)	α_t (dB/m)
Nonradiative Guide (Alumina) $a/\lambda_0=0.45$	$\sqrt{\epsilon_r-1}\,b/\lambda_0=0.45$	15	8.99	3.08	20.68	1.02
		30	4.50	1.54	10.34	2.46
		60	2.25	0.77	5.17	6.10
		90	1.50	0.51	3.45	10.53
	$\sqrt{\epsilon_r-1}\,b/\lambda_0=0.7$	15	8.99	4.80	9.49	0.71
		30	4.50	2.40	4.74	1.55
		60	2.25	1.20	2.37	3.47
		90	1.50	0.80	1.58	5.61
Insular Guide (Alumina) $a/b=2.0$		15	5.34	2.68	9.55	0.93
		30	2.68	1.34	4.76	2.24
		60	1.34	0.67	2.37	5.54
		90	0.90	0.45	1.58	9.55

parallel to the conductor surfaces. Similar reduction of loss has also been observed in an image guide with the polarization parallel to the ground plane [10].

VI. Coupling Coefficient

Couplers are important in millimeter-wave applications. Fig. 8 shows coupled strips or a double-strip guide [11]. The coupling coefficient between the strips is given by

$$c=(\beta_e-\beta_o)/2 \tag{6}$$

where β_e and β_o are phase constants of the even and odd modes in the double-strip guide. Characteristic equations for β_e and β_o can be found elsewhere [11]. In Fig. 9, coupling coefficients are plotted as function of the spacing for two special cases. On the ordinate of the right side, the normalized length L_c/λ_0 required for 0-dB coupling is marked. A 3-dB coupler needs only half of this length.

VII. Preliminary Measurements

Since the fields in the strip resemble those of a rectangular metal waveguide as shown in Fig. 4, most waveguide components may be simulated with nonradiative guides, as well. To confirm this, some qualitative, rather than quantitative, measurements were made at 50 GHz by using polystyrene strips, 2.7 mm in width and 2.0 mm in thickness. Though strips as thick as 3.3 mm would be better, only the thinner ones were available. Fig. 10 shows strip components fabricated for measurement. The guide wavelength is calculated to be 11.2 mm long and the transmission loss to be 3.76 dB/m.

The strips were tapered for 10-mm length at each end in the H plane and held between two square brass plates, 5

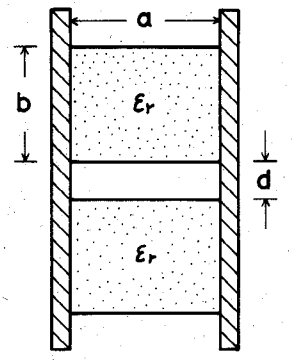

Fig. 8. Cross-sectional view of coupled strips or double-strip guide.

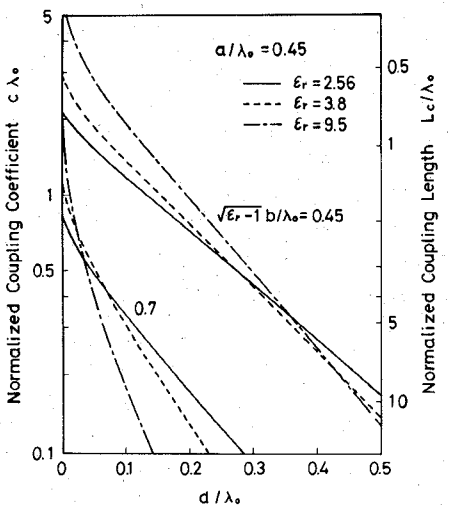

Fig. 9. Normalized coupling coefficient and normalized 0-dB coupling length for coupled strips of alumina ($\epsilon_r = 9.5$), fused quartz ($\epsilon_r = 3.8$), and polystyrene ($\epsilon_r = 2.56$).

cm × 5 cm. The tapered sections were made to stick out to facilitate transition from rectangular metal waveguides to dielectric strips. Even though horns were not used in the present measurements, no serious trouble occurred. Insertion losses and couplings of the components were measured by the substitution method by using a straight strip as the standard of comparison along with various other strips.

A. T-Junction

A small chip of polystyrene was attached just above the intersection of the junction for enhancing coupling between each arm. Though its properties have not yet been understood thoroughly, the chip is expected to act as a matching element like a stub in a metal waveguide. By carefully adjusting the length of the chip at 4 mm, we could obtain 4.2-dB coupling between the main and stub ends, and 5.3-dB coupling between both ends of the main arm. Further improvement can be expected if the chip is adjusted more precisely.

B. Right-Angle Corner

Two chips, 3.5 mm in length, were attached symmetrically as extensions of the arms. An insertion loss of about 1.8 dB was observed. The corner seems much more frequency sensitive than the T-junction, since the insertion loss critically depends on the chip length.

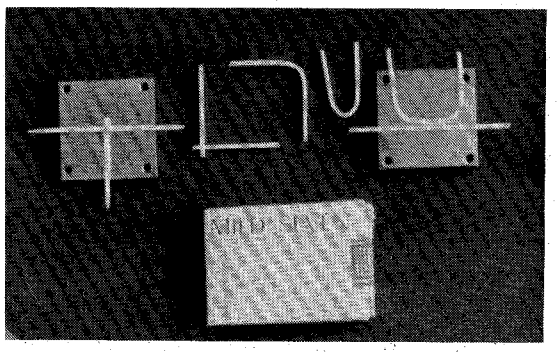

Fig. 10. Photograph of various strip structures of polystyrene tested. Left to right, T-junction, right-angle corner, 90° bend, 180° bend, and directional coupler.

C. 90° and 180° Bends

Since bends are basic components in millimeter-wave circuits, 90° and 180° bends with a radius of curvature of 10 mm were fabricated and tested. Insertion loss of the 90° bend was found to be 0.3 dB. When the 180° bend was set in the measuring system for the standard straight strip, reflection affected circuit matching. But, after the *E–H* tuners were readjusted, no insertion loss could be observed. The 180° bend seems to act as a heavily reactive component rather than a simple bend, because the radius of curvature is as small as one guide wavelength.

D. Directional Coupler

Referring to Fig. 9, a 0-dB directional coupler was designed with 16-mm length of coupling and 1-mm spacing. The coupled strip was sharply bent by 90° at both ends of the coupling region. The main port and the reversely coupled port were provided with film absorbers to achieve reflection-free termination. By carefully adjusting the spacing between the two strips, a forward coupling of 0.18 dB was obtained.

VIII. Conclusion

Basic properties of a nonradiative guide have been discussed. The guide has proved to be quite practical, since the bandwidth is wide enough to fully cover the *U* band or the *V* band and the transmission loss is less than that of the insular guide. Furthermore, measurements confirm that radiated waves are almost completely suppressed.

Bends, junctions, and a directional coupler were fabricated and successfully tested at 50 GHz to demonstrate their usefulness. An efficient transition between a metal waveguide and a nonradiative guide is a primary need. We are developing a theory to better understand the performance of the guide and to facilitate the design of various useful circuit components.

Acknowledgment

The authors wish to thank M. Shimokoriyama and M. Ando for their assistance in computation and measurements.

REFERENCES

[1] T. Itoh, "Inverted strip dielectric waveguide for millimeter-wave integrated circuits," *IEEE Trans. Microwave Theory Tech.*, vol. MTT-24, pp. 821–827, Nov. 1976.

[2] R. M. Knox, "Integrated circuits for the millimeter through optical frequency range," in *Proc. Symp. Submillimeter Waves*, pp. 497–516, 1970.

[3] J. E. Kietzer, A. R. Kaurs, and B. J. Levin, "A V-Band communication transmitter and receiver system using dielectric waveguide integrated circuits," *IEEE Trans. Microwave Theory Tech.*, vol. MTT-24, pp. 297–803, Nov. 1976.

[4] T. Itoh and B. Adelseck, "Trapped image guide for millimeter-wave circuits," *IEEE Trans. Microwave Theory Tech.*, vol. MTT-28, pp. 1433–1436, Dec. 1980.

[5] F. J. Tischer, "A waveguide structure with low losses," *Arch. Elec. Übertragung*, vol. 7, pp. 592–596, Dec. 1953.

[6] ——, "H guide with laminated dielectric slab," *IEEE Trans. Microwave Theory Tech.*, vol. MTT-18, pp. 9–15, Jan. 1970.

[7] R. E. Collin, *Field Theory of Guided Waves*. New York: McGraw-Hill, 1960, ch. 11, pp. 470–473.

[8] J. W. E. Griemsmann and L. Birenbaum, "A low-loss H-guide for millimeter wavelengths," in *Proc. Symp. Millimeter Waves*, pp. 543–562, 1959.

[9] R. M. Knox, "Dielectric waveguide microwave integrated circuits—An overview," *IEEE Trans. Microwave Theory Tech.*, vol. MTT-24, pp. 806–814, Nov. 1976.

[10] S. Shindo and T. Itanami, "Low-loss rectangular dielectric image line for millimeter-wave integrated circuits," *IEEE Trans. Microwave Theory Tech.*, vol. MTT-26, pp. 747–751, Oct. 1978.

[11] R. F. B. Conlon and F. A. Benson, "Propagation and attenuation in the double-strip H guide," *Proc. Inst. Elec. Eng.*, vol. 113, pp. 1311–1320, Aug. 1966.

Tsukasa Yoneyama (S'60–M'69) graduated from Tohoku University, Sendai, Japan, in 1959, and received the M.E. and Ph.D. degrees in electrical communication engineering from the same university in 1961 and 1964, respectively.

He is currently an Associate Professor at the Research Institute of Electrical Communication, Tohoku University, where his research interests are concerned with electromagnetic field theory and millimeter-wave integrated circuits.

Dr. Yoneyama is a member of IECE of Japan.

Shigeo Nishida (SM'59) was born in Nagoya, Japan, on March 7, 1924. He graduated from Tohoku University, Sendai, Japan, in 1949, and received the Ph.D. degree from the same university in 1959.

He was appointed a Research Associate and an Associate Professor at the Research Institute of Electrical Communication, Tohoku University, in 1949 and 1955, respectively. From 1957 to 1959, on leave of absence from Tohoku University, he joined the Microwave Research Institute of the Polytechnic Institute of Brooklyn, Brooklyn, NY, where he was engaged in the research on microwave waveguides and antennas. Since 1964, he has been a Professor at Tohoku University, and his major interests are in microwave and optical-wave transmissions.